12-1994

Localization of individual calcium channels at the release face of a presynaptic nerve terminal

Philip G. Haydon
Iowa State University

Eric Henderson
Iowa State University, telomere@iastate.edu

Elis F. Stanley
National Institutes of Health

Neuron, Vol. 13, 1275–1280, December, 1994, Copyright © 1994 by Cell Press

Localization of Individual Calcium Channels at the Release Face of a Presynaptic Nerve Terminal

Philip G. Haydon,* Eric Henderson,* and Elis F. Stanley†
*Department of Zoology and Genetics
Laboratory of Cellular Signaling
Room 339, Science II
Iowa State University
Ames, Iowa 50011
†Synaptic Mechanisms Section
Room 5-A-27, Building 36
National Institute of Neurological Disorders and Stroke
Division of Intramural Research
National Institutes of Health
Bethesda, Maryland 20892

Summary

Studies using biophysical techniques suggest a highly structured organization of calcium channels at the presynaptic transmitter release face (Llinás et al., 1981; Stanley, 1993), but it has not as yet proved possible to localize identified channels at the required nanometer level of resolution. We have used atomic force microscopy on the calyx-type nerve terminal of the chick ciliary ganglion to localize single calcium channels tagged via biotinylated ω-conotoxin GVIA to avidin-coated 30 nm gold particles. Calcium channels were in low (modal value approximately ≤ 1 per μm²) and high (modal value ≈ 55 per μm²) density areas and exhibited a prominent interchannel spacing of 40 nm, indicating an intermolecular linkage. Particles were observed in clusters and short linear or parallel linear arrays, groupings that may reflect calcium channel organization at the transmitter release site.

Introduction

Recent physiological findings on the presynaptic nerve terminal release face by combined patch-clamp and transmitter detection (Stanley, 1993) or the identification of protein components associated with secretory vesicle docking (Bennett et al., 1992; Lévêque et al., 1992, 1994; O'Connor et al., 1993; Yoshida et al., 1992; Mastrogiacomo et al., 1994; Abe et al., 1993) suggest that calcium channels are an integral part of a multimolecular transmitter release mechanism. Although these channels have been localized to the nerve terminal release face by fluorescent stains (Robitaille et al., 1990; Cohen et al., 1991; Torri Tarelli et al., 1991), patch-clamp recording (Stanley, 1991), and detection of calcium entry (Llinás et al., 1992; Smith et al., 1993), it has not proved possible to demonstrate their spatial distribution at the single-channel level. We have examined the transmitter release face surface topography and distribution of calcium channels by atomic force microscopy (AFM) applied to the calyx-type presynaptic nerve terminal of the chick ciliary ganglion. AFM is a surface topography scanning technique with nanometer resolution that, in contrast to electron microscopy, can be used to scan hydrated biological samples (Henderson et al., 1992; Parpura et al., 1993a, 1993b; Butt et al., 1990; Hoh et al., 1991; Hoh and Hansma, 1992). Most nerve terminals are of such small size that, once isolated in a hydrated state, their surfaces are highly curved and difficult to study in detail with a contact scanning technique such as AFM. In contrast, the chick ciliary ganglion calyx synapse is extraordinary for its sheet-like presynaptic terminal that can completely envelope the postsynaptic ciliary neuron (Figure 1A) (Hess, 1965; de Lorenzo, 1960; Landmesser and Pilar, 1972; Stanley, 1992). This nerve terminal has been used previously to record whole-terminal calcium currents (Stanley, 1989; Martin et al., 1989; Stanley and Goping, 1991; Yawo and Momiyama, 1993) and transmitter release site-associated single calcium channels (Stanley, 1991, 1993). The isolated calyx nerve terminal has a flat and extensive transmitter release face that is particularly favorable for direct examination with AFM.

Results and Discussion

Preparation of Nerve Terminals for AFM

Chick ciliary ganglia were dissociated enzymatically and plated on polylysine-coated coverslips, and calyx nerve terminals were identified under the light microscope by the attached axon and by staining with 4-Di-2-Asp (Figures 1B and 1C) as described (Stanley and Goping, 1991; Stanley, 1991). The location of each calyx was recorded by noting its position relative to the coordinates of an electron microscopy grid attached to the underside of the coverslip and by a sketch of the surrounding terrain (see Experimental Procedures). The preparation was then fixed and transferred to the atomic force microscope.

AFM Scanning of Nerve Terminals

At low gain, the calyx was seen as a flat extension of the axon (Figure 1D; Figure 2C), and in some cases, the release face was identified clearly from its spoon-like structure. The transmitter release face was in general smooth without any obvious surface features except gentle undulations (Figure 1E). Terminals that were dehydrated and scanned in air exhibited numerous small round structures of 91–170 nm that were particularly evident at the very thin fringes of the calyx. These were attributed to secretory vesicles that became apparent when the surface membrane collapsed onto the cytoplasmic components (Figure 1F), since they were not seen in axons, neuronal cell bodies, or glial cells. The unexpected large size of these vesicles can be attributed mostly to the overlying plasma membrane and dehydrated cytoplasmic components.

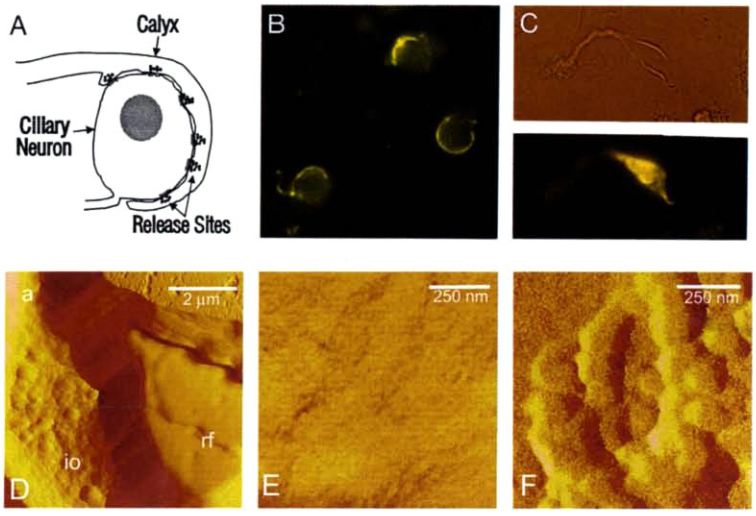

Figure 1. Structure of Calyx-Type Synapse as Seen by Light Microscopy and AFM

(A) Diagram of the calyx–ciliary neuron synapse. The nerve terminal forms a sheet that envelops the postsynaptic ciliary neuron.

(B and C) Staining (4-Di-2-Asp) of dissociated ciliary ganglia showing ciliary neurons with attached nerve terminals (B) and an isolated calyx that has adhered to the coverslip (C).

(D and E) AFM scans of a calyx fragment (D). The axon (a) spreads out into the calyx, which would normally surround the ciliary neuron (see [A]). The left edge of the calyx has been cut open to reveal intracellular organelles (io), and the presumed transmitter release face (rf) is seen within the bowl of the calyx. Note the generally smooth release face surface scanned at high gain in (E).

(F) Fringe of a calyx dehydrated in an alcohol series. The spherical structures were suggestive of secretory vesicles overlaid by the surface membrane. Hydrated samples were scanned in PBS (D and E), and dehydrated samples were scanned in air (F).

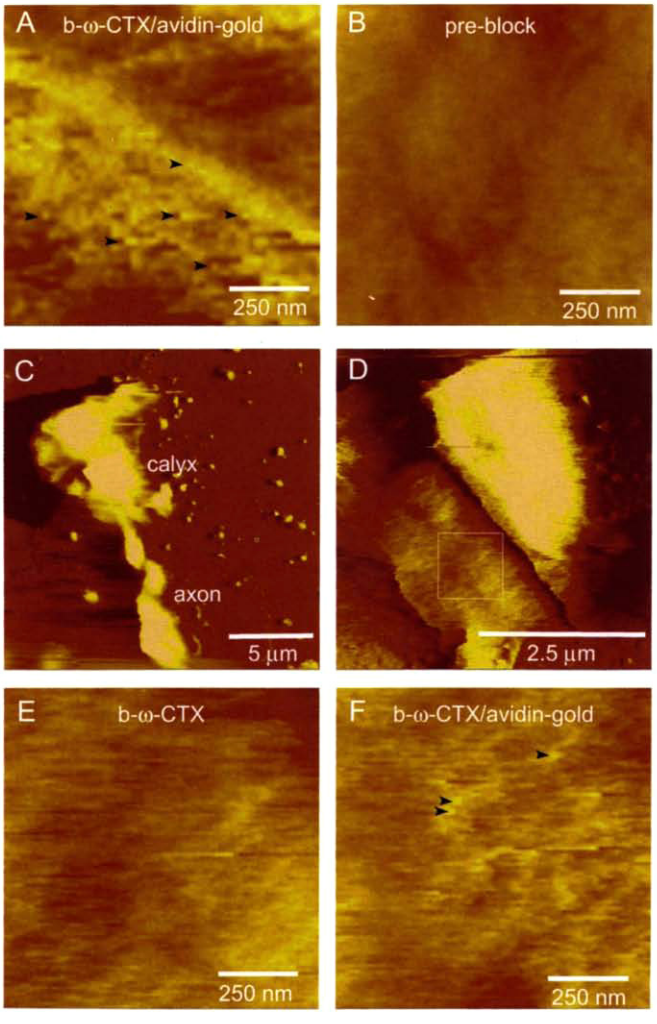

Figure 2. Binding of Gold Particles to Calcium Channels

(A and B) 1 μm^2 area of b-ω-CTx/gold (A) and ω-CTx preblocked (B) calyx scans. Examples of particles are indicated by arrowheads. There were 67 particles in this field, most of which were in the lower left region. Note regions with both high and low particle densities in (A) and the absence of particles in (B).

(C–F) b-ω-CTx-treated terminal scanned before and after avidin–gold.

(C) Low magnification image of the axon and attached nerve terminal prior to gold.

(D) Higher power view (5 × 5 μm) showing axon attachment site and proximal calyx.

(E) Enlargement (1 μm^2) of area boxed in (D).

(F) Same area as in (E) after avidin–gold. This is a relatively low gold particle density area; 3 particles are indicated by arrowheads. Terminals preblocked with ω-CTx (50 μg/ml for 15 min; n = 4) exhibited no particles in the post scan. All images were scanned under PBS.

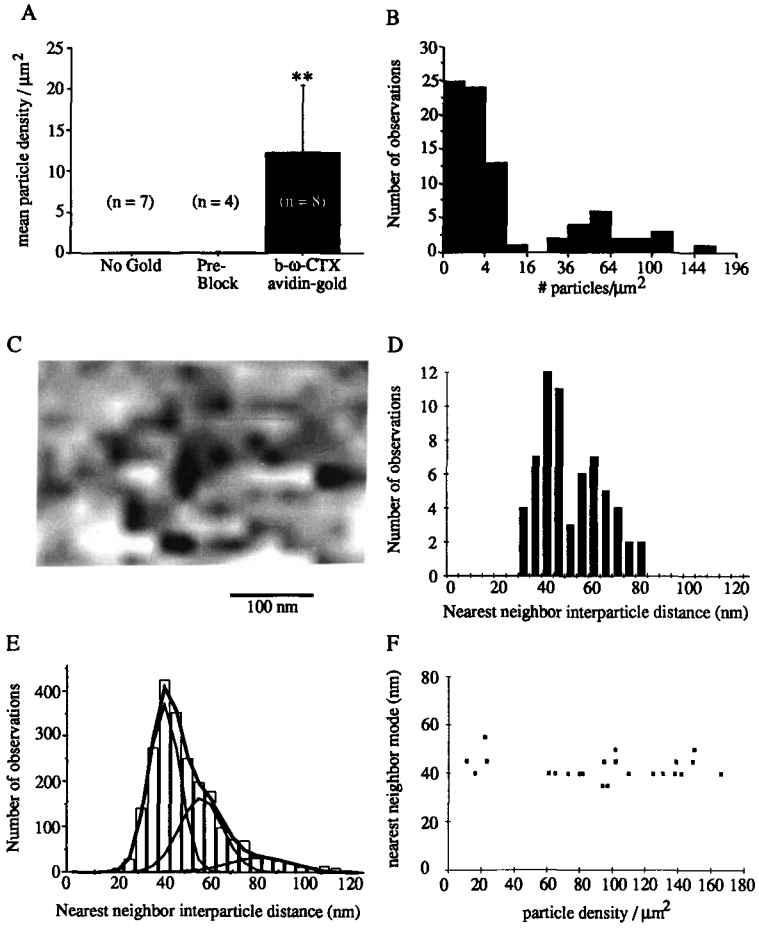

Figure 3. Analysis of Gold Particle Distribution

(A) Histogram of particle density in no-gold (pooled untreated and b-ω-CTx-treated, prior to avidin-gold), preblocked (ω-CTx followed by b-ω-CTx/avidin-gold), and test b-ω-CTx/avidin-gold-treated nerve terminal areas. A high quality 5 × 5 μm scan was selected for each terminal. The scans were randomized and analyzed blind. Each 5 × 5 μm scan was divided into 1 μm² areas, and the number of particles in each area was counted and averaged. The test values were compared with the pooled counts of terminals scanned without gold treatment. All scanned areas of the terminals were included in this comparison, without selecting for putative release face areas. The particle density was significantly higher in the gold-treated calyces (asterisks, $p < .01$ versus either control group, Mann-Whitney U test).

(B) Frequency histogram of particle density per 1 μm² field. The histogram is composed of two nonoverlapping distributions of particles at low (<16 particles per μm²) and high (>16 particles per μm²) density.

(C) The central region of Figure 2A after background smoothing and enhanced and reversed contrast to facilitate visualization of the gold particles. The apparent particle widths may be larger than 30 nm owing to a convolution of the scanning tip and the particle edges. However, this exaggerated fringe of sharp-edged objects, characteristic of AFM, does not affect the localization of the particle centers (Vasenka et al., 1994).

(D–E) Frequency histograms of particle nearest-neighbor distances. The coordinates of the center of each particle in the scan were determined, and a computer program was used to calculate the center-to-center distance from each particle to its nearest neighbor.

(D) An example from a single 1 μm² field (65 particles).

(E) Pooled data of 2273 particles in 24 1 μm² regions from two nerve terminals is fit by the sum of three Gaussian distributions with modal values of 39.9, 56.0, and 81.6.

(F) Plot of modal nearest-neighbor distance, binned as in (D), for 23 1 μm² fields against the number of particles in the field (squares). The nearest-neighbor analysis was made from the same data set as the analysis in (A) and (B) but not identical 1 μm² fields.

Localization of Calcium Channels with ω-Conotoxin

We searched for calcium channels by tagging the channels with colloidal gold particles via ω-conotoxin GVIA (ω-CTx), a toxin that irreversibly blocks both transmission and virtually all the presynaptic calcium current (Stanley and Goping, 1991; Stanley and Atrakchi, 1990; Yawo and Momiyama, 1993) at this synapse. The test calyx terminals were incubated with biotinylated ω-CTx (b-ω-CTx) followed by 30 nm avidin-gold particles. Three types of controls were used: untreated, b-ω-CTx treated without gold, and preblocked. In the latter, we first blocked the toxin binding sites with untagged ω-CTx and followed this with the complete b-ω-CTx/avidin-gold treatment. There was a visually obvious difference in the AFM scans of the test and control terminals. Low power scans of test terminals exhibited a "roughness" (Figure 2A) that was never observed in controls (Figure 2B). At high gain, this was found to be due to round structures attached to the surface membrane with diameters that were consistent with gold particles. Particle density was counted blind. Densities were high in test terminals (12.20 ± 8.24 particles per μm²; mean ± SEM; n = 8) but not in controls (0.09 ± 0.05 particles per μm²; n = 7; Figure 3A). A b-ω-CTx-treated nerve terminal was scanned both before and after avidin-gold (Figures 2C–2F). Particles were detected only in the latter, confirming that they were associated with colloidal gold treatment and were not simply topographical features of the nerve terminal. Gold particles detected in the test preparations were bound specifically to calcium channels, since they were absent in preparations preblocked with native toxin (Figure 2B; Figure 3A).

Analysis of Calcium Channel Distribution

We examined calcium channel distribution by determining gold particle density in 1 μm² membrane areas. This ranged from 1 to >150 particles per μm². A frequency histogram plot gave two distinct peaks with high (>16 particles per μm²) and low (<16 particles

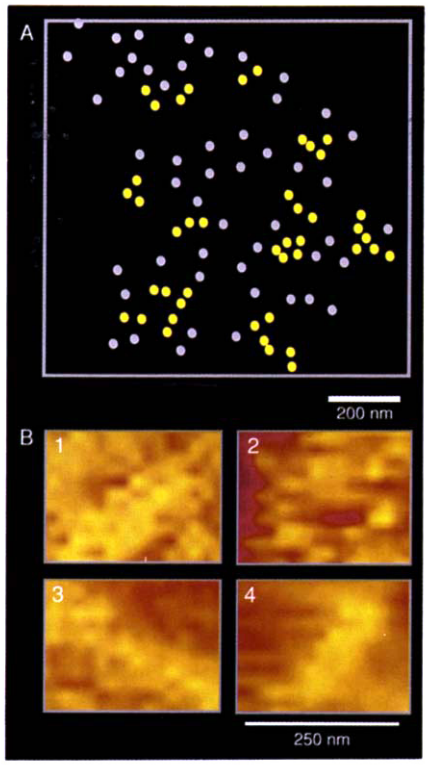

Figure 4. Particle Clusters and Arrays

(A) Particle distribution overlay from one high density 1 μm² field. Particles with center-to-center nearest-neighbor distances of <50 nm (peak from Figure 3D) are highlighted in yellow. A linear array of 4 particles is present in the cluster on the lower left.

(B) Particle arrays on the release face of the nerve terminal scanned in PBS. Panel 1, parallel linear; panel 2, circular; panels 3 and 4, linear arrays. Of these, the linear array was the most common.

per μm²) particle densities (Figure 3B). These findings are consistent with single calcium channel recording from calyx transmitter release face in which comparable channel densities were detected and clustering was evident (Stanley, 1991).

We analyzed the particle distributions further by determining the distance from one particle to its nearest neighbor. This analysis indicated a prominent center-to-center interparticle distance of ~40 nm (Figures 3D and 3E) in virtually all fields examined. This finding was independent of total particle density in the range of 11–166 particles per μm² (Figure 3F). To test whether this spacing could happen by chance, random 30 nm particle distributions were generated with densities paired to each experimentally recorded area. None of these exhibited similar nearest-neighbor distributions with modal values similar to those observed in the experimental preparations. The 40 nm spacing was not particle diameter limited, since gold particles attached to the nerve terminal were on occasion detected as close as 30 nm. Less prominent peaks were observed at about 60 and 80 nm, raising the possibility that the minimum interchannel spacing is ~20 nm (detecting a 20 nm nearest-neighbor distance was precluded by the size of the gold particles). This interpretation is consistent with an interchannel distance equal to, or greater than, the estimated size of a single brain calcium channel (Witcher et al., 1993).

To examine the distribution of only the closely associated particles in the scan, we created a scatter diagram of all the particle centers and then highlighted those that were <50 nm from a partner (Figure 4A). This procedure eliminated many of the randomly distributed particles and effectively selected for clusters (Figures 4A and 4B). In many of these clusters, the particles were scattered randomly, but some patterns were observed. Of these, the most common was the linear array that was typically composed of 3–10 particles (modal value = 5) and had a total length of 238 ± 98 nm (mean ± SD; n = 37).

Previous studies have shown that calcium channels are located on the aspect of the nerve terminal that is opposed to the postsynaptic membrane (Robitaille et al., 1990; Cohen et al., 1991; Stanley, 1991; Llinás et al., 1992; Smith et al., 1993). Nerve terminals imaged by freeze fracture exhibited large transmembrane particles at release sites (Pumplin et al., 1981; Heuser et al., 1974, 1979; Ceccarelli et al., 1979), which were believed to reflect the transmembrane regions of calcium channels. However, many other putative membrane proteins, including syntaxin (Bennett et al., 1992; O'Connor et al., 1993; Horikawa et al., 1993), neurexin (Petrenko et al., 1991; Petrenko, 1993), and calcium-activated potassium channels (Roberts et al., 1990; Robitaille et al., 1993), are also localized at or near the transmitter release site, and these may also generate particles in the freeze-fracture replica. Release face calcium channels can be identified with light microscopy, but the results obtained with AFM represent a 10-fold improvement in resolution, down to the molecular level. The detection of a preferred modal interchannel spacing that is independent of channel density suggests that these channels are anchored to a membrane-associated latticework. This hypothetical scaffold presumably also anchors other components of the release face (e.g., Bennett et al., 1992; Lévêque et al., 1992; O'Connor et al., 1993; Yoshida et al., 1992) and may ensure, among other functions, the correct spacing between the calcium channels and the calcium binding site on the transmitter release mechanism. Such a structural link has been predicted from the finding that the quantity of calcium that enters during single calcium channel activity can be sufficient to gate individual release sites (Stanley, 1993).

Experimental Procedures

Isolation of Calyx Nerve Terminals

Chick embryo ciliary ganglia (15-day-old) were dissociated as described (Stanley and Goping, 1991; Stanley, 1991) but were incubated with enzymes for 150 min to increase the yield of isolated calyces. The preparation was plated on a poly-L-lysine-coated coverslip and incubated at 37°C in minimal essential medium

(MEM) to allow the dissociated cells to attach. The coverslip was then transferred to an inverted microscope. Nerve terminals were identified in vitro from obvious structural clues together with staining using the vital dye 4-Di-2-Asp (Magrassi et al., 1987) (Figures 1B and 1C). Previous studies that include recording release face calcium channels (Stanley, 1991) and transmitter release from individual terminals (Stanley, 1993) have established the specificity of this stain in this preparation. The location of the terminals was noted by their relation to an electron microscopy grid attached to the underside of the coverslip. A sketch was also made of the terminal and the surrounding cells and cell debris so that the calyx could be reidentified under the AFM. The preparation was then fixed in 4% paraformaldehyde in phosphate-buffered saline (PBS) and transferred to a Nanoscope III atomic force microscope (Digital Instruments) equipped with a J-scanner (125 μm maximum field size). Terminals were scanned in PBS, except in a few cases, in which they were dehydrated in an ethyl alcohol series before scanning and scanned under air. The general region containing the terminal was positioned under the tip of the scanning probe using a dissecting microscope. The calyx and surrounding structures were then located with a low power scan. On occasion, the terminal was lost prior to scanning during the treatment procedures or at an early stage in the AFM. We were therefore careful to scan only terminals that could be unequivocally reidentified by both location and shape. All images are presented in error signal mode (Putman et al., 1992).

Tagging Calcium Channels with Colloidal Gold

The dissociated preparation was treated with 4 μg/ml b-ω-CTx GVIA (Molecular Probes) in MEM for 90 min at 37°C and fixed in 4% paraformaldehyde in PBS. After extensive washing in PBS and a final wash in 50 mM glycine/PBS, the preparation was treated with 30 nm avidin-gold (1:10 dilution; EY chemicals), then washed and refixed in 2% gluteraldehyde (30 min). Preparations that were examined before and after gold treatment were scanned following the paraformaldehyde step first and were then treated with avidin-gold and fixed in gluteraldehyde.

Acknowledgments

We are grateful for the technical assistance of Robert T. Doyle and comments by Drs. Jamie Vesenka, Sheldon Shen, Vladimir Parpura, S. Brian Andrews, and Tom S. Reese. This work was supported by grants from the NIH (NS 24233 and NS 26650), the McKnight Foundation, and the NINDS intramural program NIH.

The costs of publication of this article were defrayed in part by the payment of page charges. This article must therefore be hereby marked *"advertisement"* in accordance with 18 USC Section 1734 solely to indicate this fact.

Received June 20, 1994; revised September 6, 1994.

References

Abe, T., Saisu, H., and Horikawa, H. P. M. (1993). Synaptocanalins (N-type Ca channel-associated proteins) form a complex with SNAP-25 and synaptotagmin. Ann. NY Acad. Sci. *707*, 373–375.

Bennett, M. K., Calakos, N., and Scheller, R. H. (1992). Syntaxin: a synaptic protein implicated in docking of synaptic vesicles at presynaptic active zones. Science *257*, 255–259.

Butt, H. J., Wolff, E. K., Gould, S. A., Dixon, N. B., Peterson, C. M., and Hansma, P. K. (1990). Imaging cells with the atomic force microscope. J. Struct. Biol. *105*, 54–61.

Ceccarelli, B., Grohavaz, F., and Hurlbut, W. P. (1979). Freeze-fracture studies of frog neuromuscular junctions during intense release of neurotransmitter. Effects of black widow spider venom and Ca^{2+} free solutions on the structure of the active zones. J. Cell Biol. *81*, 163–177.

Cohen, M. W., Jones, O. T., and Angelides, K. J. (1991). Distribution of Ca^{2+} channels on frog motor nerve terminals revealed by fluorescent ω-conotoxin. J. Neurosci. *11*, 1032–1039.

de Lorenzo, A. J. (1960). The fine structure of synapses in the ciliary ganglion of the chick. J. Biophys. Biochem. Cytol. *7*, 31–36.

Henderson, E., Haydon, P. G., and Sakaguchi, D. S. (1992). Actin filament dynamics in living glia imaged by atomic force microscopy. Science *257*, 1944–1946.

Hess, A. (1965). Developmental changes in the structure of the synapse on the myelinated cell bodies of the chicken ciliary ganglion. J. Cell Biol. *25*, 1–19.

Heuser, J. E., Reese, T. S., and Landis, D. M. D. (1974). Functional changes in frog neuromuscular junctions studied with freeze fracture. J. Neurocytol. *3*, 109–131.

Heuser, J. E., Reese, T. S., Dennis, M. J., Jan, Y., Jan, L., and Evans, L. (1979). Synaptic vesicle exocytosis captured by quick freezing and correlated with quantal transmitter release. J. Cell Biol. *81*, 275–300.

Hoh, J. H., and Hansma, P. K. (1992). Atomic force microscopy for high resolution imaging in cell biology. Trends Cell Biol. *2*, 208–213.

Hoh, J. H., Lal, R., John, S. A., Revel, J.-P., and Arnsdorf, M. F. (1991). Atomic force microscopy and dissection of gap junctions. Science *253*, 1405–1408.

Horikawa, H. P. M., Saisu, H., Ishizuka, T., Sekine, Y., Tsugita, A., Odani, S., and Abe, T. (1993). A complex of rab3A, SNAP-25, VAMP/synaptobrevin-2 and syntaxins in brain presynaptic terminals. FEBS Lett. *330*, 236–240.

Landmesser, L., and Pilar, G. (1972). The onset and development of transmission in the chick ciliary ganglion. J. Physiol. *222*, 691–713.

Lévêque, C., Hoshino, T., David, P., Shoji-Kasai, Y., Leys, K., Omori, A., Lang, B., El Far, O., Sato, K., Martin-Moutot, N., Newsom-Davis, J., Takahashi, M., and Seagar, M. J. (1992). The synaptic vesicle protein synaptotagmin associates with calcium channels and is a putative Lambert-Eaton myasthenic syndrome antigen. Proc. Natl. Acad. Sci. USA *89*, 3625–3629.

Lévêque, C., El Far, O., Martin-Moutot, N., Sato, K., Kato, R., Takahashi, M., and Seagar, M. J. (1994). Purification of the N-type calcium channel associated with syntaxin and synaptotagmin. A complex implicated in synaptic vesicle exocytosis. J. Biol. Chem. *269*, 6306–6312.

Llinás, R. R., Steinberg, I. Z., and Walton, K. (1981). Relationship between presynaptic calcium current and postsynaptic potential in squid giant synapse. Biophys. J. *33*, 323–351.

Llinás, R. R., Sugimori, M., and Silver, R. B. (1992). Microdomains of high calcium concentration in a presynaptic terminal. Science *256*, 677–679.

Magrassi, L., Purves, D., and Lichtman, J. W. (1987). Fluorescent probes that stain living nerve terminals. J. Neurosci. *7*, 1207–1214.

Martin, A. R., Patel, V., Faille, L., and Mallart, A. (1989). Presynaptic calcium currents recorded from calcyform nerve terminals in the lizard ciliary ganglion. Neurosci. Lett. *105*, 14–18.

Mastrogiacomo, A., Parsons, S. M., Zampighi, G. A., Jenden, D. J., Umbach, J. A., and Gundersen, C. B. (1994). Cysteine string proteins: a potential link between synaptic vesicles and presynaptic Ca^{2+} channels. Science *263*, 981–982.

O'Connor, V. M., Shamotienko, O., Grishin, E., and Betz, H. (1993). On the structure of the 'synaptosecretosome': Evidence for a neurexin/synaptotagmin/syntaxin/Ca^{2+} channel complex. FEBS Lett. *326*, 255–260.

Parpura, V., Haydon, P. G., and Henderson, E. (1993a). Three-dimentional imaging of living neurons and glia with the atomic force microscope. J. Cell Sci. *104*, 427–432.

Parpura, V., Haydon, P. G., Sakaguchi, D. S., and Henderson, E. (1993b). Atomic force microscopy and manipulation of living glial cells. J. Vac. Sci. Technol. *11*, 773–775.

Petrenko, A. G. (1993). α-latrotoxin receptor: implications in nerve terminal function. FEBS Lett. *325*, 81–85.

Petrenko, A. G., Perin, M. S., Davletov, B. A., Ushkaryov, Y. A., Geppert, M., and Südhof, T. C. (1991). Binding of synaptotagmin to the α-latroxin receptor implicates both in synaptic vesicle exocytosis. Nature *353*, 65–68.

Pumplin, D. W., Reese, T. S., and Llinás, R. R. (1981). Are the presynaptic membrane particles the calcium channels? Proc. Natl. Acad. Sci. USA *78*, 7210–7213.

Putman, C. A. J., Van der Werk, K., de Grooth, B. G., van Hulst, N. F., Greve, J., and Hansma, P. K. (1992). A new imaging mode in atomic force microscopy based on the error signal. Soc. Photo-optical Instrumenta. Eng. *1639*, 198–204.

Roberts, W. M., Jacobs, R. A., and Hudspeth, A. J. (1990). Colocalization of ion channels involved in frequency selectivity and synaptic transmission at presynaptic active zones of hair cells. J. Neurosci. *10*, 3664–3684.

Robitaille, R., Adler, E. M., and Charlton, M. P. (1990). Strategic location of calcium channels at transmitter release sites of frog neuromuscular synapses. Neuron *5*, 773–779.

Robitaille, R., Garcia, M. L., Kaczorowski, G. J., and Charlton, M. P. (1993). Functional colocalization of calcium and calcium-gated potassium channels in control of transmitter release. Neuron *11*, 645–655.

Smith, S. J., Buchanan, J., Osses, L. R., Charlton, M. P., and Augustine, G. J. (1993). The spatial distribution of calcium signals in squid presynaptic terminals. J. Physiol. *472*, 573–593.

Stanley, E. F. (1989). Calcium currents in a vertebrate presynaptic nerve terminal: the chick ciliary ganglion calyx. Brain Res. *505*, 341–345.

Stanley, E. F. (1991). Single calcium channels on a cholinergic presynaptic nerve terminal. Neuron *7*, 585–591.

Stanley, E. F. (1992). The calyx-type synapse of the chick ciliary ganglion as a model of fast cholinergic transmission. Can. J. Physiol. Pharmacol. *70* (Suppl.), 73–77.

Stanley, E. F. (1993). Single calcium channels and acetylcholine release at a presynaptic nerve terminal. Neuron *11*, 1007–1011.

Stanley, E. F., and Atrakchi, A. H (1990). The calcium current in the presynaptic nerve terminal of the chick giant synapse is insensitive to the dihydropyridine nifedipine. Proc. Natl. Acad. Sci. USA *87*, 9683–9687.

Stanley, E. F., and Goping, G. (1991). Characterization of a calcium current in a vertebrate cholinergic presynaptic nerve terminal. J. Neurosci. *11*, 985–993.

Torri Tarelli, F., Passafaro, M., Clementi, F., and Sher, E. (1991). Presynaptic localization of omega-conotoxin-sensitive calcium channels at the frog neuromuscular junction. Brain Res. *547*, 331–334.

Vasenka, J., Miller, E. R., and Henderson, E. R. (1994). Three-dimentional probe reconstruction for atomic force microscopy. Rev. Sci. Instrumenta. *65*, 2249–2251.

Witcher, D. R., De Waard, M., Sakamoto, J., Franzini-Armstrong, C., Pragnell, M., Kahl, S. D., and Campbell, K. P. (1993). Subunit identification and reconstitution of the N-type Ca^{2+} channel complex purified from brain. Science *261*, 486–489.

Yawo, H., and Momiyama, A. (1993). Re-evaluation of calcium currents in pre- and postsynaptic neurones of the chick ciliary ganglion. J. Physiol. *460*, 153–172.

Yoshida, A., Oho, C., Omori, A., Kuwahara, R., Ito, T., and Takahashi, M. (1992). HPC-1 is associated with synaptotagmin and omega-conotoxin receptor. J. Biol. Chem. *267*, 24925–24928.